Journal of Vacuum Science Technology B

Controlled removal of hydrogen atoms from H-terminated silicon surfaces

Hamed Alemansour,[1] S. O. Reza Moheimani,[1, a)] James H. G. Owen,[2] John N. Randall,[2] and Ehud Fuchs[2]
[1)]*Erik Jonsson School of Engineering and Computer Science, The University of Texas at Dallas, Richardson, TX 75080, USA*
[2)]*Zyvex Labs LLC, 1301 N Plano Rd., Richardson, TX 75081, USA*

The controlled formation of dangling bond structures on a H-terminated silicon surface is the first step in an atomically precise method of fabrication of silicon quantum electronic devices. An ultrahigh vacuum scanning tunneling microscope (STM) tip is used to selectively desorb hydrogen atoms from a Si(100)-2×1:H surface by injecting electrons with the sample held at a positive bias voltage. We propose a lithography method that allows the STM to operate under negative bias imaging conditions and simultaneously desorb H atoms as required. A high frequency signal is added to the negative bias voltage to deliver the required energy for hydrogen removal. The resulting current at this frequency and its harmonics are filtered to minimize their effect on the operation of the STM's feedback control loop. We show that the chance of tip-sample crash during the lithography process is reduced by employing this method. We also demonstrate that this approach offers a significant potential for controlled and precise removal of H atoms from a H-terminated silicon surface and thus may be used for the fabrication of practical silicon-based atomic-scale devices.

I. INTRODUCTION

Imaging at the atomic-scale is achievable by the scanning tunneling microscope (STM), an instrument that operates based on the quantum mechanical phenomenon known as tunneling[1]. An ultrahigh vacuum (UHV) STM can be employed to investigate chemical, physical, and structural properties of a surface as well as to perform lithography with atomic resolution[2]. Due to the unique role of silicon in the semiconductor industry, considerable research has been devoted to performing lithography on hydrogen-passivated Si(100) surfaces[3–8]. Hydrogen atoms can be selectively removed and replaced with specific atomic species to achieve the desired properties, thanks to the binding chemistry of silicon[9–11]. The ability to fabricate atomic scale devices and integrate them with conventional electronics on the same Si substrate makes this method a candidate technology for fabrication of next-generation electronic devices[12–14].

There are two different mechanisms for hydrogen depassivation lithography (HDL) which are represented by two distinct regimes as a function of sample bias[5,6,15]. In the high-voltage (6–10 V) regime, the electron's energy can exceed the threshold energy of the Si-H bond causing the removal of hydrogen atoms from the surface[6]. In the low-voltage regime (< 6 V), higher currents are needed for depassivation. There are also studies that report performing HDL at negative sample bias voltages[16]. Compared to the positive bias case, significantly higher bias voltages (-4 V to -10 V) and tunneling currents (1–10 nA) are required at negative voltages[16]. This can adversely affect the tip resolution[16].

The precise removal of hydrogen plays a crucial role in the fabrication of atomic scale devices. The lateral resolution in high-voltage regime is limited to approximately 5 nm[17,18]. On the contrary, resolution down to the atomic level are achievable in low-bias mode[19]. This has led to the development of feedback controlled lithography (FCL) to controllably remove one hydrogen atom at a time[4]. Upon the removal of a hydrogen atom from a H-terminated silicon surface, a sudden increase of tunneling current is observed due to the bare silicon atom's higher local density of states compared to the hydrogen. The controller compensates for this jump in the tunneling current in order to maintain the current setpoint value. Lyding used this signature of a desorption event to selectively remove single hydrogen atoms[4]. FCL works by actively monitoring the topography signal and the tunneling current, and terminating the lithography process as soon as a desorption event is detected either as a spike in the current, or a step in topography[20]. This prevents the unintentional depassivation of nearby atoms[4], and improves the lithography precision.

In conventional methods of HDL, the setpoint current and bias voltage of STM are substantially changed to switch from the imaging to the lithography mode. This alters the operating point of STM and manifests itself as a change in the low frequency gain of the system. Later in this paper, we demonstrate that the low-frequency gain of the system may more than double during this switch. Such a large variation in gain adversely affects the stability and performance of the STM for which PI gains are already tuned, and in turn increases the risk of a tip-sample crash. If the tip crashes at any point during the HDL process of a given surface or device, the entire sample is usually rendered unusable. Here, we report how depassivation of hydrogen atoms may be achieved while maintaining the set current and voltage of imaging mode. This decreases the chance of a tip-sample crash by eliminating the switching step between the two modes of operation. This is particularly effective for the removal of single H atoms, and thus we have developed the voltage-modulated feedback-controlled lithography (VMFCL) method based on Lyding's FCL method to selectively remove single hydrogen atoms.

II. EXPERIMENT AND METHODS

The experiments described here were performed at room temperature with a home built UHV STM[21] having a base pressure as low as 10^{-11} Torr. A 20-bit digital signal processor (DSP) with a sampling frequency of 100 kHz, commercially known as ZyVector, is used for control purposes.

[a)]Corresponding author: Reza.Moheimani@utdallas.edu

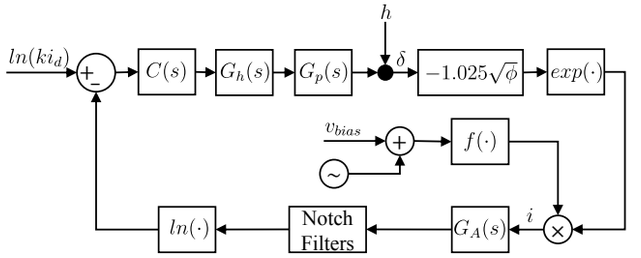

FIG. 1. Block diagram of STM Z-axis with simplified tunneling current model. $C(s)$, $G_h(s)$, $G_p(s)$, and $G_A(s)$ are controller, high voltage amplifier, Z axis actuator, and preamplifier.

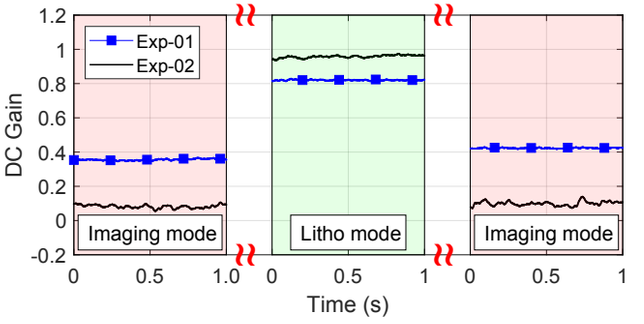

FIG. 2. DC gain changes when the STM is switched from the imaging mode to lithography mode, and *vice versa*. Exp-01 and Exp-02 show lithography at positive and negative bias voltages, respectively.

To prepare the H-terminated Si(100) sample, a $4 \times 8\,mm^2$ piece of 1 ohm-cm boron-doped wafer is cut and solvent cleaned. After introduction to UHV, the sample is degassed at 650°C for 8 hours and then is flashed to 1250°C for 30 s to remove the surface oxide film and any surface carbon contamination. This flashing is repeated 3 times, and then the surface is cooled to 350°C. To saturate the surface with H atoms, the clean Si(100) surface is exposed to a flux of atomic H from a 1300 °C tungsten filament for 4 minutes, while it is maintained at 350°C. The filament cracks the background H_2 molecules which land on it into atomic H. We have used tungsten tips in this work, which are prepared using electrochemical etching followed by field directed sputter sharpening[22].

An approximate expression for the tunneling current shows the dependence of the electrical current on the tip-sample voltage difference in addition to an exponential dependence on the tip-sample gap. This well known model is expressed as[23–25]:

$$i \approx f(v, \rho_t, \rho_s) e^{-1.025\sqrt{\phi}\delta} \tag{1}$$

In this model, f is dependent on the density of states (DOS) of the tip and the sample as well as the voltage difference between the two. Here, ϕ is the barrier height in electron volts, and δ is approximately the tip-sample gap in Ångstroms.

As the tunneling current is in the range of few nano amperes, a preamplifier with the gain of k is used to amplify the current and convert it to a measurable voltage. A block diagram of the simplified model is shown in Fig. 1. To linearize the model, the natural logarithm of the current is taken after it is amplified by the preamplifier. By taking the natural logarithm of the current, we will have access to a variable that changes linearly with the tip-sample gap. Thus, by regulating this variable we may regulate the gap, assuming that the remaining parameters are constant.

$$\ell n(ki) = \ell n(kf(v, \rho_t, \rho_s)) - 1.025\sqrt{\phi}\delta \tag{2}$$

By comparing the frequency responses of the STM obtained from successive measurements, we observed that the low-frequency gain of the open loop system is changed by varying the bias voltage or setpoint current. This is expected since in Eq. 2 the barrier height is dependent on the tunneling parameters. In [24], we showed that the STM feedback control loop could experience instabilities if this gain is increased approximately by a factor of two. Here, we measure variations in the low-frequency gain of the STM as it is switched from imaging ($V_{bias} = -2.5\,V$ and $I_{tun} = 1\,nA$) to lithography mode, and then is switched back to imaging mode. The results are shown in Fig. 2. We repeated this experiment for both lithography modes at positive ($V_{bias} = +4\,V$ and $I_{tun} = 3\,nA$) and negative ($V_{bias} = -7\,V$ and $I_{tun} = 3\,nA$) sample bias voltages, denoted by Exp-01 and Exp-02 in Fig. 2, respectively. The low-frequency gain was increased almost two times in Exp-01 and ten times in Exp-02 after switching to lithography mode. This clearly shows that the chance of control loop instability leading to a tip-sample crash is significant in conventional methods of lithography.

During normal STM operation, only low frequency current measurements play a role in the construction of the surface topography image. Considering that the normal closed-loop bandwidth of STM is only a few hundred Hertz, a large portion of the frequency band remains intact. This bandwidth may be simultaneously used for other purposes without disturbing the normal operation of the STM. This possibility motivated us to propose a method for performing HDL that enables us to eliminate the conventional switching step from imaging to lithography mode. In this approach, the lithography is performed with the parameters conventionally used during the imaging mode. To perform lithography with a negative sample bias voltage and at a normal tip-sample gap, a sinusoidal voltage with a frequency of ω is added to the setpoint DC bias voltage. The effect of this dither signal can be measured as a current with the frequency of ω and its harmonics, as expected from Eq. 1. To minimally disturb the tip height but not excite the scanner resonant dynamics, the modulation signal frequency is set to be beyond the controller bandwidth but lower than the resonance frequency of the scanner. In addition, to ensure that the controller does not respond to the dither frequency, notch filters are incorporated in the feedback loop before taking the natural logarithm of current, attenuating the current at the frequency of ω and its first few harmonics. This enables us to manipulate the bias voltage and consequently the tip-sample current without affecting the controller, ensuring that the tip-sample gap remains unchanged.

Electrons tunnels out of the newly-exposed silicon dangling bond instead of the silicon-hydrogen bond following depassi-

vation of a hydrogen atom. This results in a step change in the DC tunneling current. The controller adjusts the tip-sample distance to maintain the setpoint value, therefore the depassivation shows up as a spike in the current or a step jump in the height. The possibility of detecting an individual desorption by monitoring the current or height motivated us to design an automated hydrogen removal routine, voltage-modulated feedback-controlled lithography (VMFCL). Fig. 3 shows the process flowchart. First, the surface is scanned and the desired coordinates are selected for hydrogen removal. Then the tip is moved to the first coordinate and a high frequency voltage is added to the DC bias voltage. The dither voltage is ramped up gradually toward the final value, while the height is monitored. The height threshold (δ) is defined as a step change in the height above which an atom of hydrogen is considered to have left the surface. The height threshold should be carefully selected because a large threshold increases the possibility of missing a desorption event while a small threshold may lead to a false detection. Once a step change in the height is detected or the dither voltage amplitude has reached its final value, it is immediately ramped down to zero and the tip is moved to the next coordinate.

III. RESULTS AND DISCUSSION

To examine the effect of the modulation voltage amplitude on hydrogen depassivation, the STM tip was moved along a dimer row at a speed of 0.1 nm/s. The sample voltage is -2.5 V plus the modulated voltage. The controller adjusts the tip-sample height to maintain a 1 nA DC tunneling current. The closed-loop bandwidth of our STM is approximately 200 Hz. The modulation frequency is selected as 1 kHz, higher than the closed-loop bandwidth and lower than the first resonance frequency of the scanner. Five notch filters at 1 kHz, 2 kHz, 3 kHz, 4 kHz, and 5 kHz are incorporated into the feedback loop to attenuate the effect of the AC voltage on the measured current. Consequently, the controller output will not be affected by the modulation signal or its harmonics. This ensures the feedback loop will operate under imaging conditions. Rather than the VMFCL approach described in Fig. 3, the modulation amplitude is increased from 0 V to 1.5 V during the first 75 s and then it is kept constant at 1.5 V. Therefore, considering the -2.5 V bias voltage, the actual sample voltage varies from -4 V to -1 V when the modulation voltage ramps all the way up to its final value. Fig. 4a shows an image of the resulting topography. The tip trajectory along the dimer row is shown with a green rectangle, moving from left to right. The first depassivation occurs when the tip has moved about 5.7 nm along the dimer row. At this point, the amplitude of the modulation voltage has reached 1.15 V. Fig. 4b shows the measured current after the notch filters as well as the modulation voltage amplitude as a function of time. Depassivation events cause spikes in the current signal. The first spike occurs at about 57 s, which matches the location of the first depassivation in the STM image. Frequent subsequent depassivations happened along the tip's path after the first depassivation, which is evident in Fig 4, showing that the modulation voltage amplitude has reached the necessary threshold needed for the depassivation. The current spike close to t=100 s is noticeably larger than others. Close examination of the experimental results reveals that this is due to an unexpected sudden decrease in the tip-sample gap. The controller remains stable, however, and quickly compensates for this drop in height.

Fig. 5(a) and 5(b) show single hydrogen removal from the H-terminated silicon surface using the VMFCL method. The sample bias voltage and the setpoint tunneling current are set to -2.5 V and 1 nA, respectively. Once the tip reaches a desired position, a 1 kHz modulation voltage is added to the setpoint bias voltage and the amplitude ramps up from zero to 1.5 V over 10 seconds. As a depassivation is detected or the modulation amplitude reaches its maximum value, the ampli-

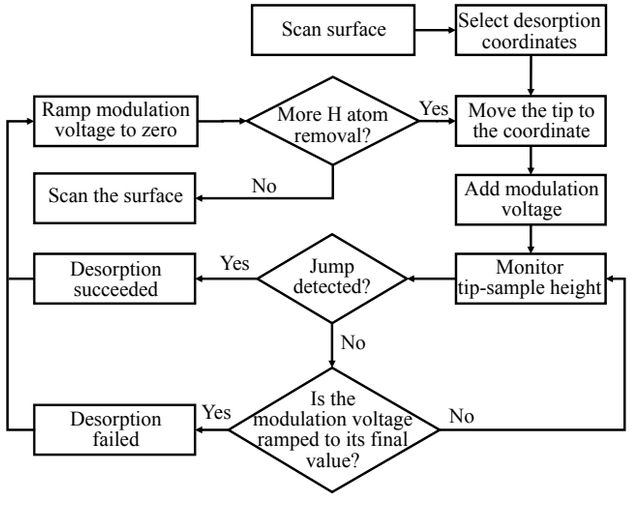

FIG. 3. Automated hydrogen removal process using VMFCL.

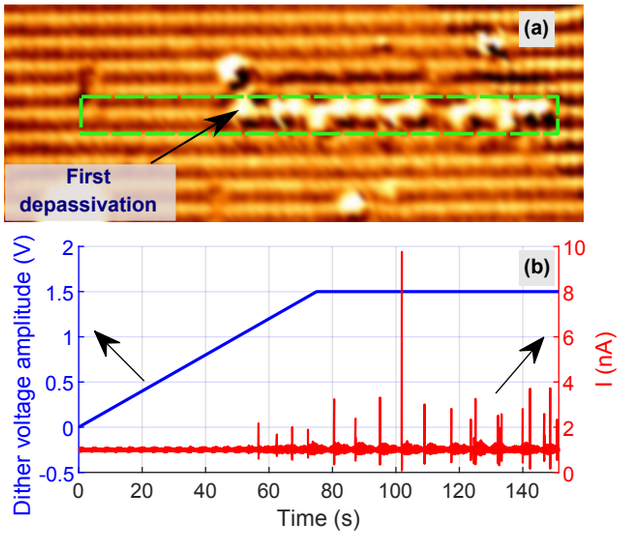

FIG. 4. (a) STM image after lithography. The tip path is shown by a green rectangle, moving from left to right. (b) The dither voltage amplitude and the filtered current.

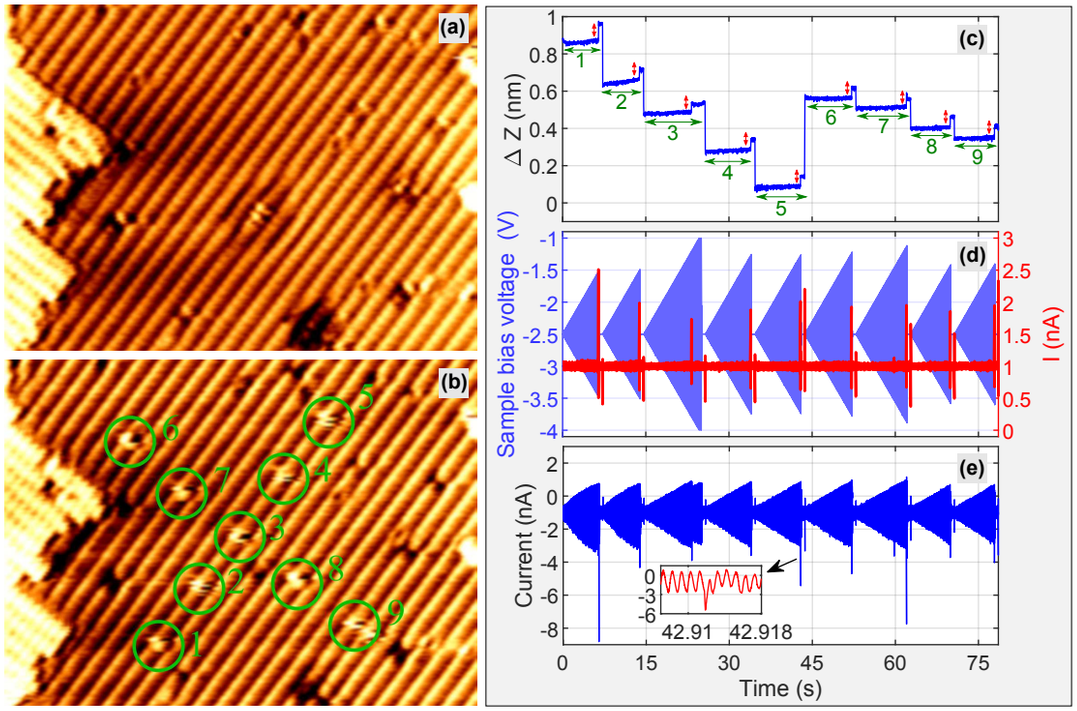

FIG. 5. The STM image of a Si(100)-2 × 1:H passivated surface (a) before and (b) after depassivation using VMFCL. Each desorption event is numbered in (b) and its corresponding displacement in the Z direction is shown by the same number in (c). Also, the tunneling current (d) after and (e) before the notch filters are measured. The removal of a hydrogen atom is detected as a jump in the current or the height.

tude ramps down to zero in 0.1 seconds. The height signal is averaged for 20 ms before being compared with the height threshold (δ), which increases the accuracy of jump detection by reducing the noise. The threshold for a jump to be considered a successful desorption event is set to 0.3 Å. As shown in Fig. 5(b), all the hydrogen atoms have been precisely removed from the surface using this method. The displacement of the Z positioner is also shown in Fig. 5(c) in which depassivation events are shown with red arrows. The current increases as soon as a hydrogen atom leaves the surface and the controller moves the tip further away from the sample to maintain the setpoint current. This step jump in the height is used to identify the desorption event. The current after the notch filters and the sample bias voltage are shown in Fig. 5(d). We observe that all depassivation events were identified except for the third one. The bias voltage modulation amplitude ramps down to zero as soon as a hydrogen atom leaves the surface and the tip is moved to the next coordinate, where another jump appears in the current and height. This jump can be associated with changes in tip-sample height as the tip moves to the new location and is not related to hydrogen depassivation. Whenever a hydrogen atom desorbs from the surface, the amplitude of the modulation bias voltage has a value in the range of 1 V to 1.5 V. The current before the notch filters is also shown in Fig. 5(e). As explained earlier, adding a modulation to the sample bias voltage induces oscillations with the same frequency in the current. Oscillations are not visible in the figure because their period is relatively small compared to the scale of the X-axis. In the inset of Fig. 5(e), there is a zoomed view showing a depassivation event. Current oscillations due to the application of the modulated voltage and the current jump resulting from the hydrogen atom removal are clearly visible in the inset.

IV. CONCLUSIONS

By adding a high-frequency voltage modulation to the DC setpoint, we were able to develop an alternative method for STM-based HDL at room temperature. This method can be implemented on most STM systems with a small modification to their software. This method has two advantages over conventional HDL. First, we were able to perform lithography on H-terminated Si while maintaining a well-controlled tip-sample distance using a negative sample bias voltage as in imaging conditions. This enhanced stability would reduce the probability of tip crashes and increase the tip's lifetime. Second, the early results of this method of HDL indicate a higher spatial resolution than conventional HDL as the exposure when moving slowly along a dimer row as in Fig. 4 is typically single H atoms, rather than whole dimers. An automated workflow for the removal of single H atoms was also implemented, which was used to create near-perfect dangling bond structures at room temperature by selectively removing single H atoms at predefined locations. Precise removal of single hydrogen atoms may enable fabrication of devices with atomically precise features, e.g. identical qubits for quantum computation[26]. The throughput of this method can also be im-

proved by integrating it with parallel STM tips[27,28], bringing the next-generation electronics into existence. Having demonstrated proof-of-principle of this lithography method, more research is needed to fully understand the underlying physics, to explore practical applications, and to determine the yield and the error rate associated with this technique. Varying the amplitude and frequency of the voltage modulation, the effect of having the modulated voltage be positive for a short time each cycle, and the speed of the tip motion may all have an effect on the size of the exposure zone and the depassivation efficiency. Furthermore, this method may also be applicable to other material systems, such as Cl-terminated Si(100) surfaces described by Dwyer and co-authors[29], selective removal of H atoms from adsorbed molecules such as PH_3, or other systems where the standard HDL method is ineffective.

ACKNOWLEDGMENTS

This material is based upon work supported by the U.S. Department of Energy's Office of Energy Efficiency and Renewable Energy (EERE) under the Advanced Manufacturing Office Award No. DE-EE0008322.

This report was prepared as an account of work sponsored by an agency of the United States Government. Neither the United States Government nor any agency thereof, nor any of their employees, makes any warranty, express or implied, or assumes any legal liability or responsibility for the accuracy, completeness, or usefulness of any information, apparatus, product, or process disclosed, or represents that its use would not infringe privately owned rights. Reference herein to any specific commercial product, process, or service by trade name, trademark, manufacturer, or otherwise does not necessarily constitute or imply its endorsement, recommendation, or favoring by the United States Government or any agency thereof. The views and opinions of authors expressed herein do not necessarily state or reflect those of the United States Government or any agency thereof.

[1] G. Binnig, H. Rohrer, Ch. Gerber, and E. Weibel. Surface studies by scanning tunneling microscopy. *Phys. Rev. Lett.*, 49:57–61, Jul 1982.

[2] M. A. Walsh and M. C. Hersam. Atomic-scale templates patterned by ultrahigh vacuum scanning tunneling microscopy on silicon. *Annual Review of Physical Chemistry*, 60(1):193–216, 2009.

[3] Ph. Avouris, R. E. Walkup, A. R. Rossi, T.-C. Shen, G. C. Abeln, J. R. Tucker, and J. W. Lyding. STM-induced H atom desorption from Si(100): isotope effects and site selectivity. *Chemical Physics Letters*, 257(1):148 – 154, 1996.

[4] M. C. Hersam, N. P. Guisinger, and J. W. Lyding. Silicon-based molecular nanotechnology. *Nanotechnology*, 11(2):70–76, June 2000.

[5] J. W. Lyding, T.-C. Shen, J. S. Hubacek, J. R. Tucker, and G. C. Abeln. Nanoscale patterning and oxidation of H-passivated Si (100)-2× 1 surfaces with an ultrahigh vacuum scanning tunneling microscope. *Applied physics letters*, 64(15):2010–2012, 1994.

[6] J. W. Lyding, G. C. Abeln, T.-C. Shen, C Wang, and J. R. Tucker. Nanometer scale patterning and oxidation of silicon surfaces with an ultrahigh vacuum scanning tunneling microscope. *Journal of Vacuum Science & Technology B: Microelectronics and Nanometer Structures Processing, Measurement, and Phenomena*, 12(6):3735–3740, 1994.

[7] Ph. Avouris, R. E. Walkup, A. R. Rossi, H. C. Akpati, P. Nordlander, T.-C. Shen, G. C. Abeln, and J. W. Lyding. Breaking individual chemical bonds via STM-induced excitations. *Surface Science*, 363(1):368 – 377, 1996.

[8] J. A. Dagata, J. Schneir, H. H. Harary, C. J. Evans, M. T. Postek, and J Bennett. Modification of hydrogen-passivated silicon by a scanning tunneling microscope operating in air. *Applied Physics Letters*, 56(20):2001–2003, 1990.

[9] D. P. Adams, T. M. Mayer, and B. S. Swartzentruber. Selective area growth of metal nanostructures. *Applied Physics Letters*, 68(16):2210–2212, 1996.

[10] M. J. Butcher, F. H. Jones, and P. H. Beton. Growth and modification of Ag islands on hydrogen terminated Si(100) surfaces. *Journal of Vacuum Science & Technology B: Microelectronics and Nanometer Structures Processing, Measurement, and Phenomena*, 18(1):13–15, 2000.

[11] R. Basu, N. P. Guisinger, M. E. Greene, and M. C. Hersam. Room temperature nanofabrication of atomically registeredheteromolecular organosilicon nanostructures using multistepfeedback controlled lithography. *Applied Physics Letters*, 85(13):2619–2621, 2004.

[12] R. Achal, M. Rashidi, J. Croshaw, D. Churchill, M. Taucer, T. Huff, M. Cloutier, J. Pitters, and R. A. Wolkow. Lithography for robust and editable atomic-scale silicon devices and memories. *Nature communications*, 9(1):2778, 2018.

[13] M. Fuechsle, J. A. Miwa, S. Mahapatra, H. Ryu, S. Lee, O. Warschkow, L. C. Hollenberg, G. Klimeck, and M. Y. Simmons. A single-atom transistor. *Nature nanotechnology*, 7(4):242, 2012.

[14] M. Y. Simmons, S. R. Schofield, J. L. O'Brien, N. J. Curson, L. Oberbeck, T. Hallam, and R. G. Clark. Towards the atomic-scale fabrication of a silicon-based solid state quantum computer. *Surface Science*, 532-535:1209 – 1218, 2003.

[15] I. W. Lyo and P. Avouris. Field-induced nanometer- to atomic-scale manipulation of silicon surfaces with the STM. *Science*, 253(5016):173–176, 1991.

[16] K. Stokbro, C. Thirstrup, M. Sakurai, U. Quaade, Ben Yu-Kuang Hu, F. Perez-Murano, and F. Grey. STM-induced hydrogen desorption via a hole resonance. *Phys. Rev. Lett.*, 80:2618–2621, Mar 1998.

[17] T. C. Shen, C. Wang, G. C. Abeln, J. R. Tucker, J. W. Lyding, Ph. Avouris, and R. E. Walkup. Atomic-scale desorption through electronic and vibrational excitation mechanisms. *Science*, 268(5217):1590–1592, 1995.

[18] L. Soukiassian, A. J. Mayne, M. Carbone, and G. Dujardin. Atomic-scale desorption of H atoms from the $\mathrm{Si}(100)-2\times1:\mathrm{H}$ surface: Inelastic electron interactions. *Phys. Rev. B*, 68:035303, Jul 2003.

[19] J. N. Randall, J. H. Owen, J. Lake, and E. Fuchs. Next generation of extreme-resolution electron beam lithography. *Journal of Vacuum Science & Technology B*, 37(6):061605, 2019.

[20] M. Møller, S. P. Jarvis, L. Guérinet, P. Sharp, R. Woolley, P. Rahe, and P. Moriarty. Automated extraction of single H atoms with STM: tip state dependency. *Nanotechnology*, 28(7):075302, January 2017.

[21] J. W. Lyding, S. Skala, J. S. Hubacek, R. Brockenbrough, and G. Gammie. Variable-temperature scanning tunneling microscope. *Review of scientific instruments*, 59(9):1897–1902, 1988.

[22] S. W. Schmucker, N. Kumar, J. R. Abelson, S. R. Daly, G. S. Girolami, M. R. Bischof, D. L. Jaeger, R. F. Reidy, B. P. Gorman, J. Alexander, J.B. Ballard, J. N. Randall, and J. W. Lyding. Field-directed sputter sharpening for tailored probe materials and atomic-scale lithography. *Nature communications*, 3(1):1–8, 2012.

[23] B. Voigtländer. *Scanning probe microscopy*. Springer, 2015.

[24] F. Tajaddodianfar, S. O. R. Moheimani, E. Fuchs, and J. N. Randall. Stability analysis of a scanning tunneling microscope control system. In *2017 American Control Conference (ACC)*, pages 204–209, May 2017.

[25] N. D. Lang. Apparent barrier height in scanning tunneling microscopy. *Phys. Rev. B*, 37:10395–10398, Jun 1988.

[26] L. Livadaru, P. Xue, Z. Shaterzadeh-Yazdi, G. A. DiLabio, J. Mutus, J. L. Pitters, B.C. Sanders, and R. A. Wolkow. Dangling-bond charge qubit on a silicon surface. *New Journal of Physics*, 12(8):083018, August 2010.

[27] J. N. Randall, J. H. Owen, J. Lake, R. Saini, E. Fuchs, M. Mahdavi, S. R. Moheimani, and B. C. Schaefer. Highly parallel scanning tunneling microscope based hydrogen depassivation lithography. *Journal of Vacuum Science & Technology B*, 36(6):06JL05, 2018.

[28] A. Alipour, M. B. Coskun, and S. O. R. Moheimani. A high bandwidth microelectromechanical system-based nanopositioner for scanning tunneling microscopy. *Review of Scientific Instruments*, 90(7):073706, 2019.

[29] K. J. Dwyer, M. Dreyer, and R. E. Butera. STM-induced desorption and lithographic patterning of Cl-Si(100)-(2x1), 2018.